On-Chip Parylene-C Microstencil for Simple-to-Use Patterning of Proteins and Cells on Polydimethylsiloxane

Donghee Lee[†] and Sung Yang*[,†,‡,§]

[†]Department of Medical System Engineering, [‡]School of Mechatronics, [§]Department of Nanobio Materials and Electronics, Gwangju Institute of Science and Technology (GIST), 123 Cheomdan-gwagiro, Buk-gu, Gwangju 500-712, Republic of Korea

S *Supporting Information*

ABSTRACT: Polydimethylsiloxane (PDMS) is widely used as a substrate in miniaturized devices, given its suitability for execution of biological and chemical assays. Here, we present a patterning approach for PDMS, which uses an on-chip Parylene-C microstencil to pattern proteins and cells. To implement the on-chip Parylene-C microstencil, we applied SiO*x*-like nanoparticle layers using atmospheric-pressure plasma-enhanced chemical vapor deposition (AP-PECVD) of tetraethyl orthosilicate (TEOS) mixed with oxygen. The complete removal of Parylene-C from PDMS following application of SiO*x*-like nanoparticle layers was demonstrated

by various surface characterization analysis, including optical transparency, surface morphology, chemical composition, and peel-off force. Furthermore, the effects of the number of AP-PECVD treatments were investigated. Our approach overcomes the tendency of Parylene-C to peel off incompletely from PDMS, which has limited its use with PDMS to date. The on-chip Parylene-C microstencil approach that is based on this Parylene-C peel-off process on PDMS can pattern proteins with 2-μm resolution and cells at single-cell resolution with a vacancy ratio as small as 10%. This provides superior user-friendliness and a greater degree of geometrical freedom than previously described approaches that require meticulous care in handling of stencil. Thus, this patterning method could be applied in various research fields to pattern proteins or cells on the flexible PDMS substrate.

KEYWORDS: *protein patterning, cell patterning, flexible substrate, polydimethylsiloxane (PDMS), Parylene-C, atmospheric-pressure plasma-enhanced chemical vapor deposition (AP-PECVD)*
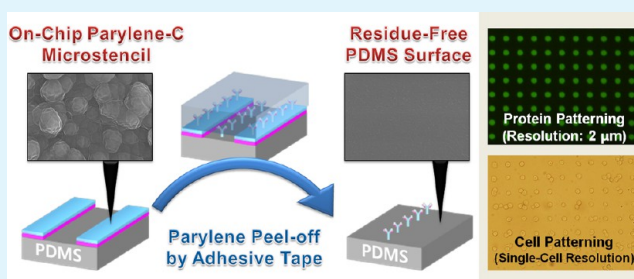
1. INTRODUCTION

Miniaturized device technology allows precise manipulation of biomolecules and cells in a microenvironment and is critical to the continued advances that enable biochips, biosensors, and "lab-on-a-chip" devices to execute biological and chemical assays on microdevices.[1,2] The precise control facilitated by this technology opens doors to new high-content and high-throughput experimental approaches for use in biomedical diagnostics, drug discovery, and tissue engineering.[3] Selective immobilization of a biomolecule on a substrate is essential for these applications; thus, a wide variety of patterning methods have been proposed to immobilize biomolecules on designated regions on substrates.[4,5] Polydimethylsiloxane (PDMS) is widely used as a substrate in such applications because it is inexpensive, easy-to-fabricate, biocompatible, self-sealable, highly elastic, and transparent.[6] Moreover, it has an innate cell-repellent property[7] that allows for easy region-specific patterning of cells. However, the tendency of PDMS to swell in the presence of organic solvents,[8] as well as the innate nanopores in the PDMS surface,[9] both limit the application of PDMS with respect to conventional patterning methods on inorganic substrates. Among these, only a few methods are available for protein patterning, including microcontact

printing,[10] patterning by microfluidic channels,[11,12] and stencil methods.[13−21] Microcontact printing with deformable PDMS stamps not only suffers from the pairing and sagging that limits the capacity for dimensional and geometrical patterning, but the drying step that is frequently part of the printing process is undesirable insofar as it compromises protein bioactivity.[22] Patterning by microfluidic channels is not routinely feasible due to complex experimental setup requirements, along with the limited capacity to accommodate various dimensional and geometrical requirements.[23]

Recently, the application of the stencil method has gained popularity owing to its suitability for patterning on PDMS, using a shadow mask made from either a PDMS sieve,[13] a Parylene-C film,[14−17] a silicon membrane,[18−20] or stainless steel.[21] The benefits of the stencil method are its capacity for reuse and the fact that it usually (with the exception of stainless steel stencils) allows micro/nanoscale patterning. However, maintaining stencil for reuse requires a cleaning process that involves washing with hazardous substances such as sulfuric

acid/hydrogen peroxide or removal of remaining biomolecules by treatment with oxygen plasma. Moreover, meticulous care is required in handling the stencil, given that the Si/SiNx membrane is fragile[18] and the polymeric membranes are very thin and deformable.[16] In addition, the monolithic structure of the stencil restricts its application to a separated pattern. In previous approaches that used Parylene-C film as a stencil, Parylene-C layers thicker than 10 μm were required to fabricate a Parylene-C stencil on a Si wafer for a durable removal process using tweezers; thus, an expensive two-step fabrication process was needed to deposit or etch the aluminum layer to provide a metal mask on the Parylene-C layer for subsequent etching of the Parylene-C layer. Considering the pros and cons of the stencil method, a disposable on-chip microstencil fabricated at low cost and using a simplified method would be a practical alternative to maximize user-friendliness and minimize maintenance for biologically oriented users.

Here, we present a simple-to-use patterning approach for PDMS that involves peeling-off of a Parylene-C layer as a disposable, on-chip microstencil on PDMS. The approach permits region-specific immobilization of proteins or cells with a greater degree of geometrical freedom; that is, by applying our method with the on-chip parylene microstencil, both separate shape and connected shape of the pattern can be realized since the on-chip parylene microstencil can be peeled off by adhesive tape regardless of the pattern's connectivity. However, the previous stencil methods can implement only the separate patterns depending on the monolithic structure of stencil. The Parylene-C peel-off method provides a chemically inert, pinhole-free, swelling-resistant, and biocompatible mechanical method of peeling that leaves no residue.[24] The process has been used with glass or silicon wafers but is not amenable to use with PDMS, given that penetration of the deposited Parylene-C layer into the innate nanopores in the PDMS surface (more than 200 nm in depth)[9] results in incomplete removal of the Parylene-C layer due to mechanical failure caused by the abrupt increase in interfacial force at the nanopores. Thus, Parylene-C deposition on PDMS has been mainly used to permanently fill gas-permeable nanopores on PDMS surfaces, to suppress the absorption of small molecules, or to increase air-sealing performance.[9,25−27]

To overcome this difficulty in implementing the Parylene-C peel-off process on PDMS, we investigated application of atmospheric-pressure plasma-enhanced chemical vapor deposition (AP-PECVD) layers to prevent the penetration of Parylene-C into the nanopores of PDMS. We used extremely rough SiOx-like nanoparticle layers,[28] which was applied using AP-PECVD of tetraethyl orthosilicate (TEOS)-O_2. The residue-free removal of Parylene-C from PDMS was verified using various surface characterization methods. The removal process of Parylene-C layer from PDMS could be implemented simply by the use of adhesive tape without any reduction in the advantageous material properties of PDMS. This provided microscale resolution and placed no geometrical restrictions on protein patterning. Using this method, we demonstrated region-specific patterning of proteins and cells with single-cell resolution. Our success can be attributed to the difference in cell-binding affinity between innately cell-repellent PDMS and selectively immobilized cell-adhesive molecules. This patterning method on flexible PDMS substrate could be used in various fusion applications, considering that PDMS is one of the most popular substrates in micrototal analysis systems and flexible

electronics[29] and the most suitable substrate in tissue engineering for mechanical stimulus of cells.[30]
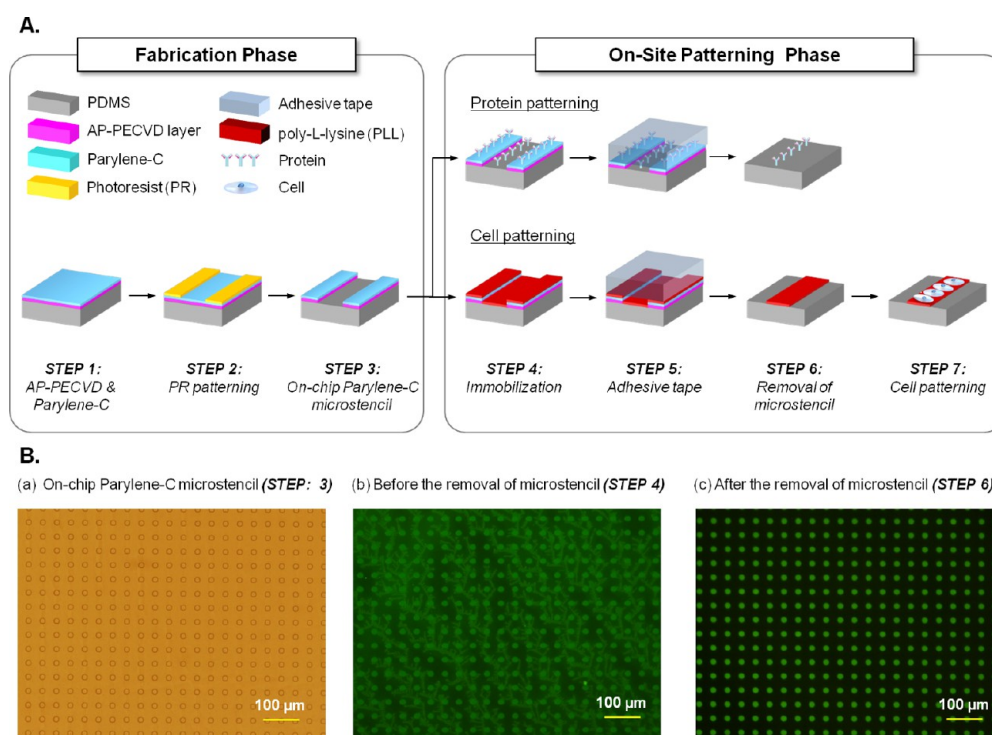
2. EXPERIMENTAL SECTION

2.1. Materials. Sylgard 184, a PDMS kit that contains two components (a liquid silicone rubber and a curing agent), was purchased from Dow-Corning Corporation (Midland, MI). Glass slides were supplied by Corning Inc. (Corning, NY). Photoresist (AZ1512) and photoresist developer (MIF300) were supplied by Clariant Corp. (Somerville, NJ). Parylene-C dimer (DPX-C) was supplied by Specialty Coating Systems Inc. (Indianapolis, IN). Buffered oxide etchant (BOE) was obtained from JT Baker (Center Valley, PA). Ethanol was purchased from Merck (Darmstadt, Germany). Skim milk was purchased from BD Biosciences (San Diego, CA). Tetraethyl orthosilicate (TEOS), fluorescein isothiocyanate (FITC)-labeled streptavidin (SA-FITC), FITC-labeled poly-L-lysine (PLL-FITC), protein G, human IgG, and FITC-labeled antihuman IgG were all purchased from Sigma-Aldrich Company (St. Louis, MO). Rhodamine-labeled antirabbit IgG, phosphate-buffered saline (PBS), RPMI 1640 medium, fetal bovine serum (FBS), and penicillin−streptomycin were all purchased from Life Technologies (Carlsbad, CA). Adhesive tape was obtained from 3 M (Saint Paul, MN).

2.2. Fabrication Phase. PDMS prepolymer and curing agent (Sylgard 184) were mixed in a 10:1 ratio, stirred, and degassed in a vacuum desiccator. Then, 20 g portions of this mixture were poured into 4 in. polystyrene Petri dishes to form a layer with a 1 mm thickness, degassed in a vacuum desiccator to remove bubbles, and cured in an oven at 80 °C for 90 min. Subsequently, the flat PDMS samples were cut into 2 × 4 cm pieces, peeled off the dishes, and placed onto a glass slide. A commercial atmospheric-pressure plasma system that used IDP-1000 (APPlasma Co., Republic of Korea) and operated at a radiofrequency (RF) of 13.56 MHz was used to deposit SiOx-like nanoparticle layers by AP-PECVD of TEOS-O_2. Helium was used as a carrier gas with 15 slm (standard liter per minute), and a mixture of TEOS (vaporized by 1 slm of argon) and O_2 with 100 sccm (standard cubic centimeter per minute) was used. An RF power of 200 W was employed for plasma deposition. The distance between the nozzle head of the plasma source and the sample was adjusted to 2 mm. The samples were mounted on a moving stage positioned below the plasma source, and the stage was moved at a speed of 20 mm/s in the orthogonal direction with respect to the plasma source head. The substrate was repeatedly passed back and forth across the plasma head region for the specified number of AP-PECVD treatments. This surface modification on the PDMS sample could be completed within 1 min.

A thin film of Parylene-C was deposited onto the AP-PECVD-treated PDMS substrates on a glass slide using PDS 2010 (Specialty Coating Systems Inc., Indianapolis, IN). The Parylene-C dimer (2.0 g) was consumed to form a Parylene-C film with a thickness of approximately 1.5 μm. Standard photolithography and reactive ion etching (RIE) were applied to pattern Parylene-C on PDMS. Briefly, a 1.8 μm-thick photoresist layer (AZ1512) was spun at 3000 rpm for 30 s. Then, it was thermally treated at 100 °C for 2 min and exposed to UV light (15 mJ/(cm²·s)) for 10 s by the use of a mask aligner, before being developed with MIF-300 developer for 40 s. The exposed Parylene-C layers in the open region of the photoresist pattern were completely etched using the RIE system (A-Tech System Co., Republic of Korea) in an O_2 plasma at 100 W for 300 s. Subsequently, PDMS samples were dipped in a BOE solution (HF/NH_4F 1:6, v%) for 20 s to remove the silica-like layer generated during the RIE process, so that pristine PDMS was exposed in the openings within the patterned Parylene-C.

2.3. On-Site Patterning Phase: Protein Patterning. SA-FITC, rhodamine-labeled antirabbit IgG, protein G, human IgG, and FITC-labeled antihuman IgG were each dissolved in PBS at concentrations of 100 μg·mL^{-1}. For direct patterning of SA-FITC by physical adsorption, SA-FITC solution was evenly distributed onto the O_2 plasma-treated Parylene-C-patterned PDMS sample. Then, the

Scheme 1. Representative Images of the Procedure Used to Peel Parylene-C from the Surface of PDMS for Region-Specific Immobilization of Proteins and Cells[a]

[a](A) Schematic diagram for this procedure, separated into 2 phases, viz., the fabrication phase and the on-site patterning phase. (B) Representative microscope images of patterned PDMS surfaces. (a) On-chip Parylene-C microstencil on PDMS after fabrication phase (STEP: 3), (b) PLL-fluorescein isothiocyanate (FITC) on PDMS before the removal of Parylene-C microstencil (STEP: 4), (c) Patterned PLL-FITC on PDMS after the removal of Parylene-C microstencil (STEP: 6).

substrate patterned with protein was stored at room temperature for 6 h to immobilize SA-FITC by means of physical adsorption with hydrophobic recovery of PDMS. For direct patterning of FITC-labeled antihuman IgG by immunoreaction with human IgG, which was bioconjugated onto PDMS using protein G, the protein G solution was first distributed uniformly over the entire surfaces of each of the PDMS samples. Then, PDMS samples were stored to immobilize protein G at room temperature for 6 h. The substrate containing protein G was then rinsed with PBS solution, after which human IgG solution was distributed onto the samples. The substrate was stored at room temperature for 1 h and was then again rinsed with PBS solution. After distributing FITC-labeled antihuman IgG solution, the substrate was stored at room temperature for 1 h. Then, PDMS samples were rinsed with distilled ionized water and dried under a stream of nitrogen gas. Adhesive tape was attached onto the PDMS surface to remove the on-chip Parylene-C microstencil on PDMS. After ensuring good contact between the tape and the Parylene-C-pattern by rubbing the region lightly, the adhesive tape was detached from the PDMS surface. The protein-patterned PDMS samples were analyzed using fluorescence microscopy to confirm the selective immobilization of SA-FITC or FITC-labeled antihuman IgG.

For indirect patterning with backfilling, milk protein solution (2% w/v in PBS) was evenly distributed onto the Parylene-C-patterned PDMS at room temperature for 6 h. These samples were then rinsed with PBS solution and dried under a stream of nitrogen gas. Adhesive tape was attached onto the PDMS surface to remove the on-chip Parylene-C microstencil. After distributing rhodamine-labeled anti-rabbit IgG solution, the substrate was stored at room temperature for 1 h. Subsequently, PDMS samples were rinsed with PBS solution and distilled ionized water and dried under a stream of nitrogen gas. The PDMS samples were then analyzed using fluorescence microscopy to confirm the selective immobilization of rhodamine-labeled antirabbit IgG to regions devoid of milk protein.

2.4. On-Site Patterning Phase: Cell Patterning. MCF-7 human mammary gland adenocarcinoma cells were cultured in RPMI 1640 that contained 10% heat-inactivated FBS and 1% penicillin and streptomycin at 37 °C in a humidified atmosphere of 5% CO_2/95% air. PLL-FITC was selectively immobilized onto PDMS using the direct patterning procedure, and the PLL-FITC-patterned PDMS was sterilized with ethanol (70%) before seeding cells. MCF-7 cells suspended in medium (2×10^6 cells · mL^{-1}) were then plated onto the surface. After an hour of incubation at 37 °C, the PDMS surface was rinsed with PBS.

2.5. Surface Characterization. Ultraviolet–visible spectropho-tometry (UV–vis) transmission spectra were measured using a Cary 5000 spectrophotometer (Agilent Technologies Inc., Santa Clara, CA) to determine the transmittance of PDMS samples before/after the removal process of Parylene-C from PDMS. The relative chemical composition ratio on the sample surface was analyzed using X-ray photoelectron spectroscopy (XPS), which was carried out using a MultiLab 2000 instrument (Thermo Electron Corp., Waltham, MA) with an Al-ka X-ray source.

Fourier transform infrared spectroscopy (FTIR)-attenuated total reflectance (ATR) measurements were performed using a 660-IR spectrometer (Agilent Technologies Inc., Santa Clara, CA) with a ZnSe crystal. The spectra were taken with nonpolarized light at a spectral resolution of 4 cm^{-1}. The analyzed spectra corresponded between 600 and 4000 cm^{-1}.

The topography of the modified PDMS surface was characterized using a S-4700 scanning electron microscope (SEM; Hitachi High-Tech Corp., Japan) at an acceleration voltage of 10 kV. Prior to imaging by the SEM, samples were sputter-coated with platinum for 65 s.

2.6. Measurement of Parylene-C Peel-Off Tension. Parylene-C peel-off tension was measured using AFG-ES50 tensile tester (AXIS Sensitive Co., Republic of Korea). To prepare a sample for peel-off
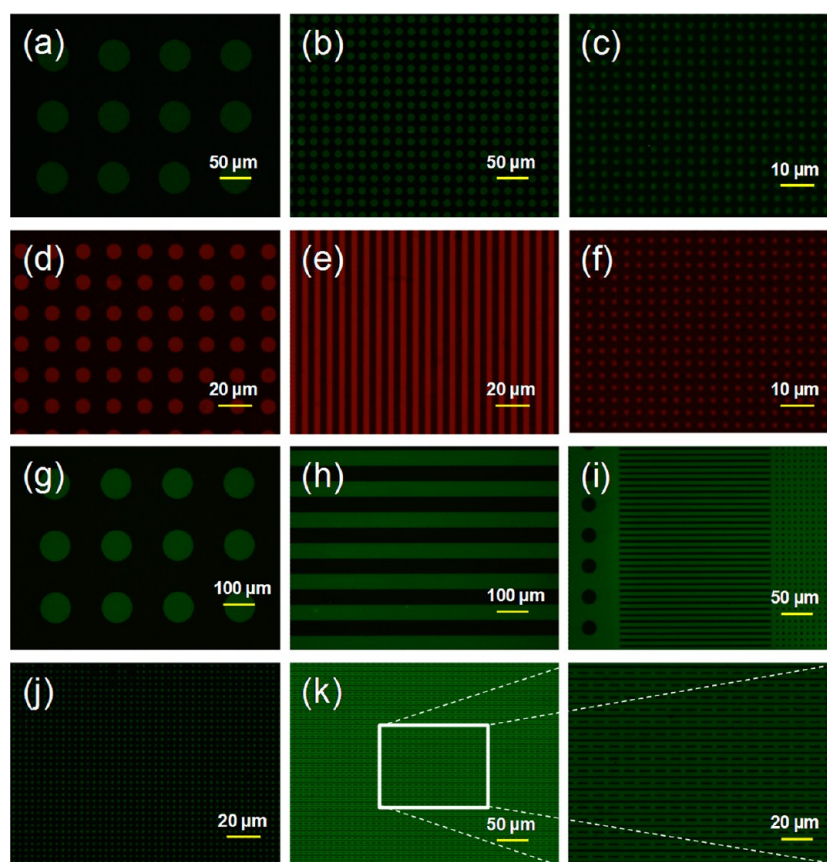
2660

dx.doi.org/10.1021/am4001166 | ACS Appl. Mater. Interfaces 2013, 5, 2658–2668

Figure 1. Fluorescence microscopy image of patterned proteins and PLL-FITC. (a–b) Patterning of FITC-labeled antihuman IgG using the direct approach. (c) Patterning of SA-FITC using the direct approach. (d–f) Patterning of rhodamine-labeled antirabbit IgG using the indirect approach. (g–k) Patterning of PLL-FITC using the direct approach.

tension measurement, the flat 1 mm-thick PDMS samples were cut into 1.5 × 3 cm pieces and permanently bonded to a glass slide by treatment with oxygen plasma. Half of each PDMS sample was covered with a cover glass. The PDMS samples were treated by AP-PECVD, depending on the condition used, and were then deposited by a Parylene-C layer. Adhesive tape was attached over the whole surface of the PDMS sample. The interface between the cover glass and PDMS at the covered section was easily opened to be fixed by a grip of tension tester. The bottom of the glass slide was attached to the mount, and the grip was moved upward at the speed of 10 mm/min. The peel-off force was recorded until the adhesive tape and PDMS sample was completely separated. The peel-off tension was measured from five samples for each AP-PECVD condition and characterized from the maximum peel-off force of each sample.

3. RESULTS AND DISCUSSION

3.1. Protein Patterning and Cell Patterning. The procedure for this patterning method on PDMS can be divided into two phases, the "fabrication phase" and the "on-site patterning phase" (Scheme 1). The "fabrication phase" includes all steps for fabricating an on-chip Parylene-C microstencil on PDMS; these processes should be executed in a clean-room facility. The "on-site patterning phase" consists of loading target proteins onto the substrates prepared in the "fabrication phase", removing on-chip Parylene-C microstencil using adhesive tape, and region-specific immobilization of cells. This "on-site patterning phase" could be performed in any on-site place where the samples are prepared, as long as adhesive tape is available. There are thus many advantages associated with this approach. The simplicity and ease with which the adhesive tape

can be attached and detached in the "on-site patterning phase" for implementing region-specific patterning of biomolecules or cells may be preferred by many biologically oriented investigators who are not familiar with fabrication processes. Moreover, the spatial temporal division of this patterning procedure into a "fabrication phase" and an "on-site patterning phase" has advantages in several aspects of application, given that biomolecules or cells could be patterned immediately prior to use on templates that have been stored long-term after the "fabrication phase".

Swelling of PDMS by organic solvents in the photolithography step can be avoided by coating PDMS with solvent-resistant Parylene-C prior to the photolithography step. At the same time, denaturation of biomolecules was prevented by mechanical removal of the on-chip Parylene-C microstencil from PDMS, thus avoiding contact between any organic solvents and biomolecules on PDMS substrates. Biomolecules can then be immobilized onto the hydrophobic PDMS surface by physical adsorption or by covalent bonding that involves various bioconjugation methods with gas phase treatment, or wet chemical methods, given the chemical inertness of the Parylene-C layer. Even though the whole surface was covered with a biomolecule solution, biomolecules could be patterned onto PDMS by applying on-chip Parylene-C microstencil on the PDMS. Through taking advantage of the innate cell-repellent property of PDMS, our method facilitates cell patterning on this flexible substrate: only cell-adhesive molecules (and not cell-repellent molecules) need to be immobilized in a region-specific manner. Cell-adhesive

molecules, such as poly-L-lysine (PLL), extracellular matrix (ECM) proteins, and peptide sequences, can be physically absorbed onto exposed areas of the Parylene-C-patterned PDMS surface; consequently, thanks to the innate capacity of PDMS to repel cells, cells will attach only to the cell-adhesive region.

We used this method to demonstrate region-specific immobilization of proteins and cells on PDMS. For protein patterning, we implemented both a direct approach to immobilize the protein on a selected region and an indirect approach with backfilling, in which the substrate was patterned with immobilization molecules and antibiofouling molecules, with micrometer resolution.[31] Figure 1 shows the patterning of proteins and PLL-FITC in various geometries and dimensions. Figure 1a−c demonstrates direct patterning of antibodies with protein G and SA-FITC, and Figure 1d−f shows indirect patterning of antibodies after adsorption of milk protein to a selected region. On the basis of the direct patterning approach, protein G, human IgG, and FITC-labeled antihuman IgG were sequentially immobilized in a circular pattern over areas with diameters of 50 μm (Figure 1a) and 10 μm (Figure 1b), and SA-FITC was immobilized in a circular pattern over an area with a diameter of 2 μm (Figure 1c). Using the indirect patterning approach, rhodamine-labeled antirabbit IgG was immobilized in circular patterns over areas with diameters of 10 μm (Figure 1d) and 2 μm (Figure 1f) and in a linear pattern with a 4 μm width (Figure 1e). Protein patterning using the indirect approach requires removal of separate on-chip Parylene-C microstencils after filling the open areas with milk protein, an antibiofouling agent; this can be achievable only by the use of adhesive tape to peel off the separate on-chip Parylene-C at once all together instead of a pair of tweezers. Figure 1g−k shows selectively immobilized PLL-FITC in a pattern that ranges from 2 to 100 μm in geometry. Separate Parylene-C microstencil can also be used to produce the connected shapes seen in the PLL-FITC patterns by utilizing adhesive tape (Figure 1i,k). Protein patterning with 2 μm resolution has been demonstrated in this study by applying photolithography. We believe that submicrometer resolution can be realized by applying E-beam lithography instead of applying conventional photolithography.

Using conventional patterning methods, it was difficult to obtain high-resolution patterning of proteins with uniformity and even more difficult on PDMS. This patterning method using an on-chip Parylene-C microstencil allowed uniform protein patterning on PDMS. For the quantitative analysis based on the fluorescence spots, the coefficient of variation (CV) was calculated to evaluate the intraspot fluorescence homogeneity and interspot fluorescence repeatability.[32] To check the uniformity of the protein patterns formed, the fluorescence signals in each circular spot in Figure 1g were measured using the ImageJ software. The circular array spots by our method presented within-spot uniformity with low CV values (less than 3.7%) as well as excellent between-spot repeatability with a low CV of mean values (3.1%) comparable to within-spot uniformity with CV values (3.1−9.6%) and between-spot repeatability with CV of mean values (3.6−8.8%) in uniform protein patterning for high-density protein micro-arrays (Figure S1a, Supporting Information).[32−34]

Cells were patterned on the innately cell-repellent PDMS by region-specific patterning of PLL-FITC as a cell-adhesive molecule with good cell-binding affinity for various cells.[35] After PLL-FITC was patterned on PDMS following removal of

Parylene-C, the PDMS surface that contained the region-specific patterned PLL-FITC was comprehensively covered with a solution that contained cells of the breast cancer cell-line MCF-7. After a 1 h incubation, autonomous immobilization of MCF-7 on PDMS was observed in the region where PLL-FITC had been immobilized; high-resolution cell patterns from μm to mm scale could be successfully generated on the PDMS surface (Figure 2). Figure 2a shows the various patterns of cells and
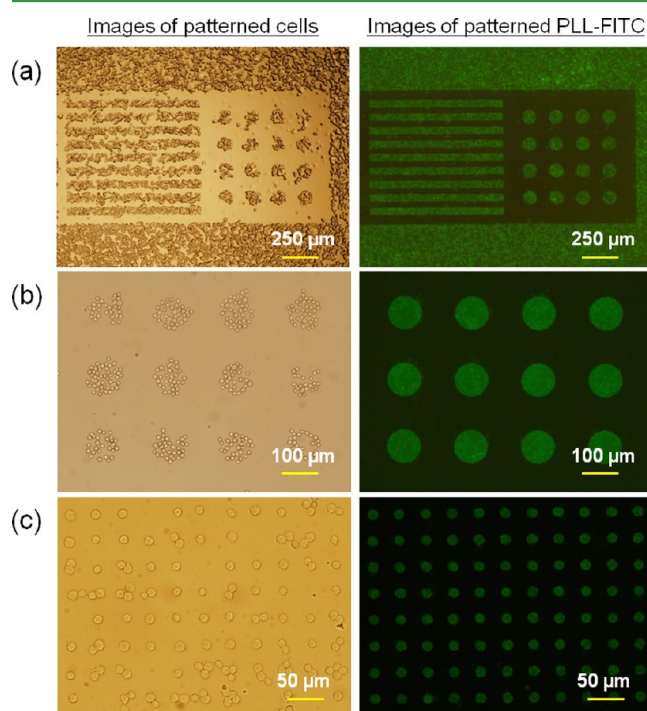

Figure 2. Microscopy image of patterned MCF-7 cells corresponding to the PLL-FITC immobilized region. (a) Linear pattern with 50 μm width and circular spot array with 100 μm diameter, as seen with a 4× objective. (b) Circular spot array with a 100 μm diameter, as seen with a 10× objective. (c) Circular spot array with a 15 μm diameter, as seen with a 20× objective.

PLL-FITC, including a linear pattern with a width of 50 μm and circular spot arrays each with diameters of 100 μm. The number of cells in a region was related to the area of the PLL-FITC-immobilized region, as shown in circular spot arrays with diameters of 100 μm (Figure 2b) and 15 μm (Figure 2c). Quantitative analysis of Figure 2c revealed that 90% of the sites were covered with cells varying from one cell to four cells (53% of the sites contains single cell only); however, the remaining 10% of the sites were vacant and contained no cells (Figure S1b, Supporting Information). This cell patterning method with single-cell resolution could be applied to a range of biological studies that require that the number of cells in a cell community and the capacity for high-throughput analysis be controlled at single-cell resolution. This capability is especially important for research that involves stem cells or tumor cells used in drug discovery where interactions between the cells in a community have profound effects on stem cell potency and tumorigenesis.[36,37]

A key advantage of the cell patterning method we describe here is the simplicity with which it can be applied using flexible PDMS substrates; only selective immobilization of cell-adhesive molecules is required owing to the innate cell-repellence of PDMS. Considering the flexibility of PDMS, the method could

2662

dx.doi.org/10.1021/am4001166 | ACS Appl. Mater. Interfaces 2013, 5, 2658−2668

be used for a variety of studies that consider cellular responses to the physical environment. This proposed cell patterning on a flexible PDMS could be utilized in various applications in tissue engineering,[30] especially when there is a need to assess the effects of externally applied mechanical deformation presented to cells as a mechanical cue, such as biomimetic stimulation of cardiac cells,[38] the regulation of stem cell differentiation,[39,40] and "organ-on-a-chip" studies.[41]

3.2. Surface Characterization on Parylene-C Removal from PDMS with AP-PECVD. The key to implementing our solvent-free PDMS-patterning method is the use of adhesive tape to completely remove the deposited Parylene-C layer from the PDMS substrate by applying an AP-PECVD process. Several studies on Parylene-C deposition on PDMS have reported penetration of Parylene-C into nanopores in the PDMS surface. The inability to completely remove the Parylene-C reduces the optical transparency, owing to the scattering of light caused by the irregular interface of residual Parylene-C on the PDMS surface. To verify the ability of our method to remove the deposited Parylene-C layer from PDMS, we used various surface characterization methods to evaluate the functionality of the SiOx-like nanoparticle layers, deposited by AP-PECVD of TEOS-O$_2$ as a precursor, to the Parylene-C peel-off process. Thus, we compared PDMS surfaces with and without AP-PECVD of TEOS-O$_2$ before and after the removal process of Parylene-C using adhesive tape from PDMS to evaluate the effectiveness of SiOx-like nanoparticle layers. Additionally, to investigate the influence of processing conditions during AP-PECVD, we analyzed the effect of varying the number of AP-PECVD treatments on the surface properties before and after the removal process of Parylene-C from PDMS (Section 3.3). The motivation for doing this is that the number of AP-PECVD treatments is related to the uniformity and thickness of SiOx-like nanoparticle layers laid down by AP-PECVD of TEOS-O$_2$. Analysis by UV−vis spectrometry revealed a marked change in optical transparency following removal process of Parylene-C from PDMS, and this depended on whether AP-PECVD had been used (Figure 3). Before removing the Parylene-C layer, the PDMS surface with
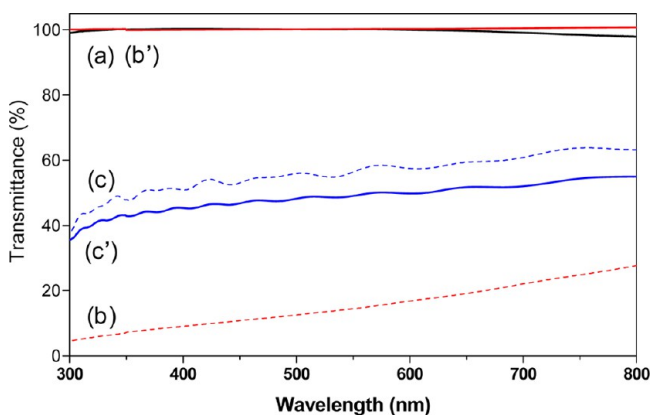

Figure 3. UV−vis transmittance spectra confirming the implementation of a complete removal of Parylene-C layer from PDMS surface by applying AP-PECVD using TEOS-O$_2$. (a) Pristine PDMS. (b) Parylene-C-deposited PDMS with AP-PECVD. (b′) Parylene-C-deposited PDMS with AP-PECVD after the removal process of Parylene-C with adhesive tape. (c) Parylene-C-deposited PDMS. (c′) Parylene-C-deposited PDMS after the removal process of Parylene-C with adhesive tape.

AP-PECVD was less transparent than that without AP-PECVD. However, whereas the transparency of the PDMS surface without AP-PECVD deteriorated after the removal process of Parylene-C, the transparency of the PDMS surface with AP-PECVD was restored to that of pristine PDMS, with fairly good transparency in the wavelength range from 300 to 800 nm.

Comparison of the surface chemical composition using XPS (Figure 4) showed that the Parylene-C layer could be
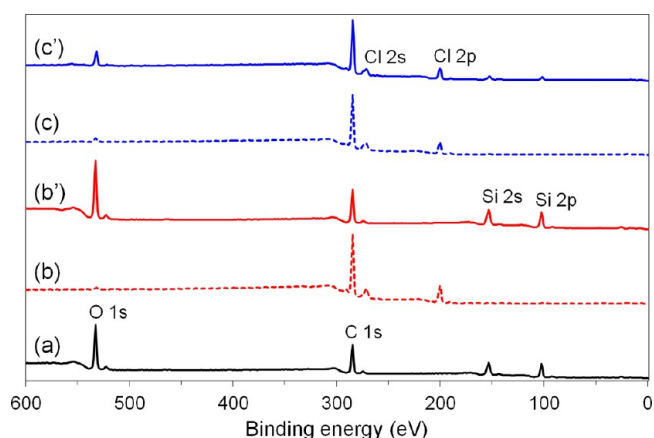

Figure 4. XPS survey spectra confirming the implementation of a complete removal of the Parylene-C layer from PDMS surface by applying AP-PECVD using TEOS-O$_2$. (a) Pristine PDMS. (b) Parylene-C-deposited PDMS with AP-PECVD. (b′) Parylene-C-deposited PDMS with AP-PECVD after the removal process of Parylene-C with adhesive tape. (c) Parylene-C-deposited PDMS. (c′) Parylene-C-deposited PDMS after the removal process of Parylene-C with adhesive tape.

completely peeled from PDMS surfaces after AP-PECVD using TEOS-O$_2$. XPS analysis demonstrated that, after Parylene-C deposition, both the PDMS surface with (Figure 4b) and without (Figure 4c) AP-PECVD showed similar peaks before the removal process of Parylene-C; however, after the removal process of Parylene-C, differences were apparent between PDMS surfaces with (Figure 4b′) and without (Figure 4c′) AP-PECVD. After the removal process of Parylene-C, the Cl 2s and Cl 2p peaks, which originate from the molecular structure of Parylene-C, were only present in PDMS without AP-PECVD (Figure 4c′), whereas the peaks of PDMS with AP-PECVD (Figure 4b′) were restored to those present in pristine PDMS (Figure 4a). Quantitative XPS analysis results confirmed the presence of a residual Parylene-C layer on PDMS that results from an incomplete removal process of Parylene-C when AP-PECVD of TEOS-O$_2$ was not performed prior to Parylene-C deposition (Figure 5).

We also compared chemical bonding on the PDMS surface using FTIR-ATR analysis. We found that the four dominant infrared peaks at the Si-(CH$_3$)$_2$ stretching mode (800 cm^{-1}), the Si−O−Si antisymmetric stretching mode (1060 cm^{-1}), the CH$_3$ symmetric deform mode (1260 cm^{-1}), and the C−H stretching mode (2900 cm^{-1}), which are observed in pristine PDMS, exist only on the PDMS with AP-PECVD after the removal process of Parylene-C (Figure 6). Thus, characterization of the chemical composition of the surface indicated complete removal of the Parylene-C layer from PDMS by applying AP-PECVD of TEOS-O$_2$. Moreover, analysis of the morphology of the PDMS surface by SEM also indicated incomplete peeling-off of the Parylene-C layer from PDMS in
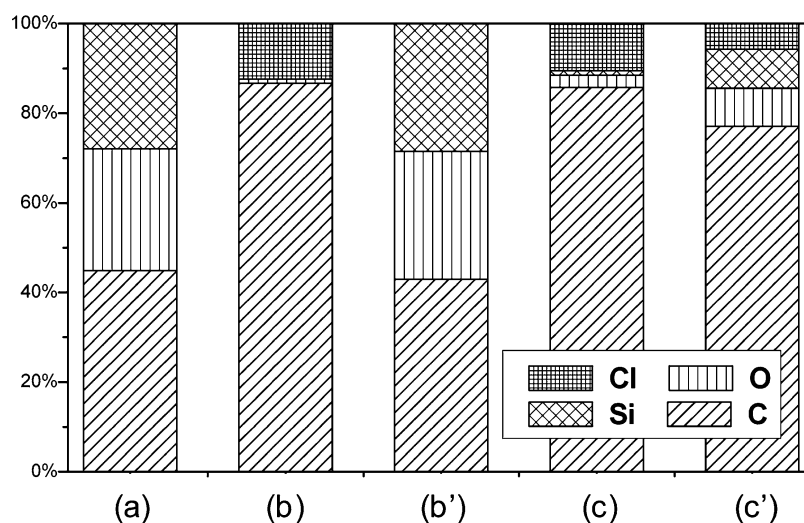
Figure 5. Chemical composition as derived by XPS analysis, confirming the implementation of a complete removal of Parylene-C layer from the PDMS surface by applying AP-PECVD using TEOS-O$_2$. (a) Pristine PDMS. (b) Parylene-C-deposited PDMS with AP-PECVD. (b′) Parylene-C-deposited PDMS with AP-PECVD after the removal process of Parylene-C with adhesive tape. (c) Parylene-C-deposited PDMS. (c′) Parylene-C-deposited PDMS after the removal process of Parylene-C with adhesive tape.
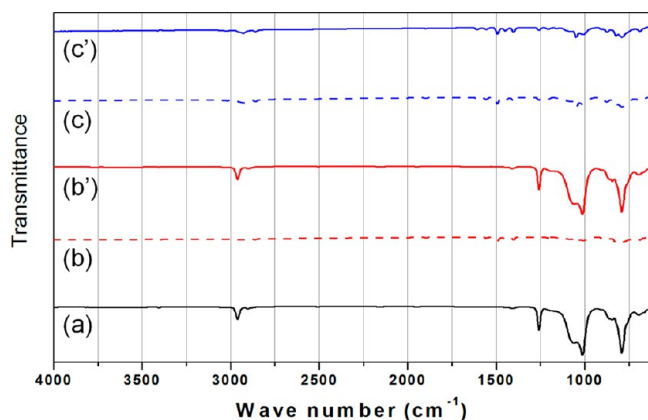

Figure 6. FTIR-ATR spectra confirming the implementation of a complete removal of Parylene-C layer from PDMS surface by applying AP-PECVD using TEOS-O$_2$. (a) Pristine PDMS. (b) Parylene-C-deposited PDMS with AP-PECVD. (b′) Parylene-C-deposited PDMS with AP-PECVD after the removal process of Parylene-C with adhesive tape. (c) Parylene-C-deposited PDMS. (c′) Parylene-C-deposited PDMS after the removal process of Parylene-C with adhesive tape.

Figure 7. SEM images confirming the implementation of a complete removal of Parylene-C layer from the PDMS surface by applying AP-PECVD using TEOS-O$_2$. (a) Pristine PDMS. (a′) PDMS deposited by AP-PECVD only. (b) Parylene-C-deposited PDMS with AP-PECVD. (b′) Parylene-C-deposited PDMS with AP-PECVD after the removal process of Parylene-C with adhesive tape. (c) Parylene-C-deposited PDMS. (c′) Parylene-C-deposited PDMS after the removal process of Parylene-C with adhesive tape.

the absence of SiOx-like nanoparticle layers deposited by AP-PECVD of TEOS-O$_2$. SEM images of the PDMS surface with AP-PECVD (Figure 7b′) reveal its close similarity to that of pristine PDMS (Figure 7a) after the removal process of Parylene-C; however, the surface morphology was maintained regardless of the removal process of Parylene-C layer if SiOx-like nanoparticle layers were not deposited before coating the Parylene-C layer (Figure 7).

Considering the similarity between pristine PDMS and the PDMS with AP-PECVD after the Parylene-C removal process in terms of chemical composition (Figure 5a,b′) and the surface morphology (Figure 7a,b′), we were curious about the fate of SiOx-like nanoparticle layers after the removal process of Parylene-C, given that it had been placed on PDMS before depositing the Parylene-C layer as shown in Figure 7a′. Through XPS analysis of the side of the peeled-off Parylene-C layer facing PDMS surfaces, we deduced that most of SiOx-like
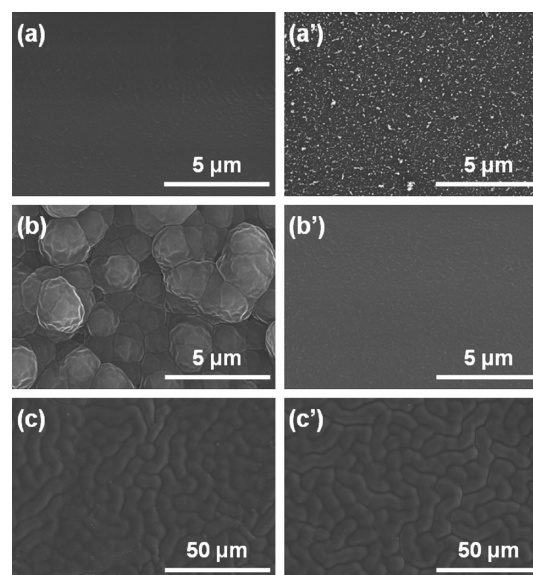
nanoparticle layers had become detached from the PDMS along with the Parylene-C layer. This conclusion was consistent with the prevalence of Si and O components in the Parylene-C layer that was peeled off from PDMS substrates with AP-PECVD (Section 3.4). Detachment of the Parylene-C layer accompanied by SiOx-like nanoparticle layers during peeling-off was inferred by the well-known capacity of Parylene-C for conformal coating.[42]

3.3. Surface Characterization by Effects of the Number of AP-PECVD Treatments.
To validate the effect of SiOx-like nanoparticle layers in implementing successful

removal of Parylene-C layer from PDMS surfaces using adhesive tape, the modified PDMS surfaces were characterized after varying the number of AP-PECVD treatments, viz., 0, 1, 3, 5, 7, or 9 depositions, prior to the removal process of Parylene-C. The thicknesses of the layers deposited on the PDMS surfaces were measured after varying the number of AP-PECVD treatments (Figure S2, Supporting Information). Regression analysis of the thicknesses of the deposited layers estimated that about 120 nm of SiOx-like nanoparticle layers in thickness was estimated to be deposited after each AP-PECVD treatment. Three physical properties of the modified surfaces were investigated to clarify the effect of AP-PECVD using TEOS-O_2 on PDMS in the removal process of Parylene-C, including peel-off tension, optical transparency, and surface topology.

The peel-off tension during the peel-off process was measured to evaluate the performance of SiOx-like nanoparticle layers in preventing the adhesion of Parylene-C to PDMS. Figure 8 shows that the peel-off tension in all cases of PDMS
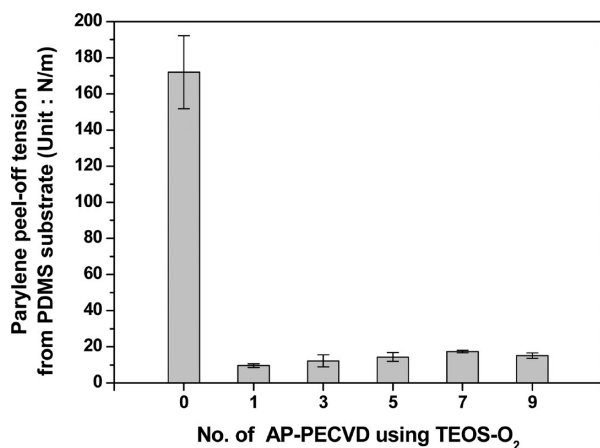

Figure 9. UV−vis transmittance spectra with variation in the number of AP-PECVD treatments (0, 1, 3, 5, 7, 9 depositions) using TEOS-O_2 to establish SiOx-like nanoparticle layers on PDMS.

Figure 8. Peel-off tension during the removal process of Parylene-C with variation in the number of AP-PECVD treatments (0, 1, 3, 5, 7, 9 depositions) using TEOS-O_2 to lay down SiOx-like nanoparticle layers on PDMS.

modified by AP-PECVD was reduced to about 10%, as compared with that of unmodified PDMS, regardless of number of AP-PECVD treatments. However, it was estimated that the mean value of peel-off force was not so linearly correlated with the number of AP-PECVD treatments, with regression analysis indicating that the sample coefficient of determination (r^2) between two variables was 0.753. SiOx-like nanoparticle layers are supposed to play a role in suppressing the penetration of Parylene-C into nanopores on the PDMS surface, resulting in a marked reduction in interfacial force in the removal process of Parylene-C.

Figure 9 shows the optical transparency in relation to the number of AP-PECVD treatments before and after the removal process of Parylene-C. Without AP-PECVD, the optical transparency of Parylene-C-deposited PDMS deteriorated after the removal process of the Parylene-C layer (empty blue squares and filled blue squares in Figure 9). In contrast, with AP-PECVD, the optical transparency of Parylene-C-deposited PDMS recovered and was similar to that of pristine PDMS after more than three times of AP-PECVD treatment; a single AP-PECVD treatment was not sufficient to completely recover transparency (empty red circles and filled red circles in
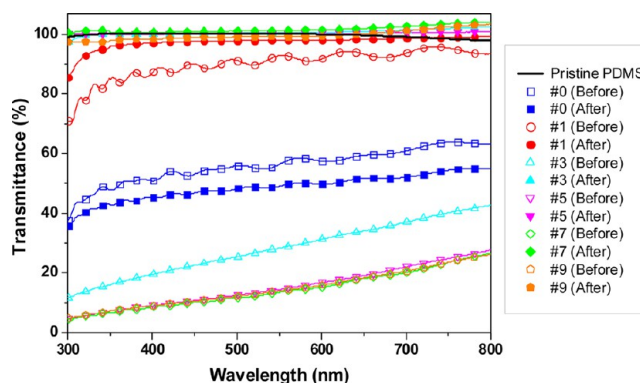
Figure 9). Although the optical transparency before the removal process of the Parylene-C layer decreased continuously with increases in the number of AP-PECVD treatments, optical transparency generally recovered after the removal process of the Parylene-C layer.

In addition, changes in the surface topography with variation of the number of AP-PECVD treatments were investigated after the Parylene-C removal process (Figure 10). Application of AP-PECVD using TEOS-O_2 as a precursor resulted in the deposition of SiOx-like nanoparticle layers on the PDMS substrate. Thus, the roughness of the surface increased proportionally with the number of AP-PECVD treatments as shown in Figure 10a. After depositing the Parylene-C layer on top of the SiOx-like nanoparticle layers on the PDMS surface (Figure 10b), the removal process of the Parylene-C layer was conducted by sequential attachment and detachment of adhesive tape. Figure 10c shows the PDMS surface after the removal process of Parylene-C without AP-PECVD (0 depositions: #0); given that the surface morphology was almost identical to a surface that had not undergone the removal process of Parylene-C, the deposited Parylene-C layer was not completely peeled off from PDMS. However, AP-PECVD using TEOS-O_2 was highly effective in removal of the Parylene-C layer from PDMS substrate (Figure 10b,c), given that there were significant changes in morphology with three or more treatments of AP-PECVD (#3−#9). This indicated that the surface morphology of peeled-off PDMS with more than three treatments of AP-PECVD was very similar to that of pristine PDMS. To ensure complete peeling-off of Parylene-C from PDMS, five treatments of deposition by AP-PECVD were used routinely in this study.

The reduced optical transparency of the Parylene-C that had been peeled off the PDMS surface without AP-PECVD compared to that of pristine PDMS can be attributed to the incomplete peeling-off of the Parylene-C layer; this was supported by analysis of the chemical composition of the surfaces, as indicated by XPS, and the surface morphology, as seen by SEM. Considering the existence of residual Parylene-C layer on the PDMS surface in the absence of SiOx-like nanoparticle layers, the internal Parylene-C layer must be peeled off by detachment of adhesive tape, given that the interfacial bonding between PDMS and penetrated Parylene-C was strong and comparable to the internal covalent bonding in the Parylene-C layer. However, in the case of AP-PECVD-treated PDMS, Parylene-C was peeled off at the interface
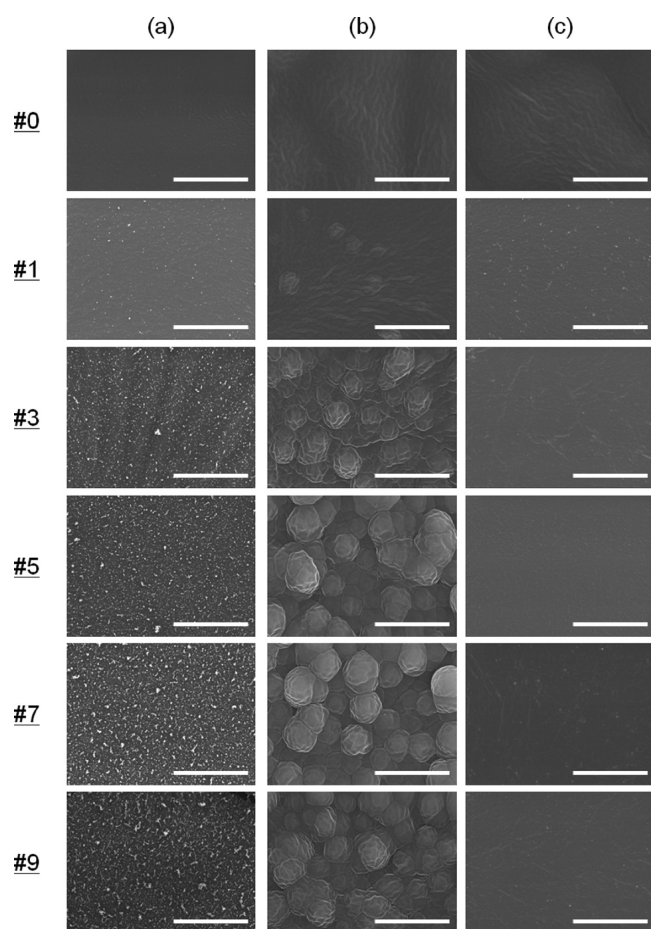
2665

dx.doi.org/10.1021/am4001166 | ACS Appl. Mater. Interfaces 2013, 5, 2658−2668

Figure 10. Comparison of SEM images generated 10 000× magnification with variation in the number of AP-PECVD treatments (0, 1, 3, 5, 7, or 9 depositions) using TEOS-O_2 to deposit SiOx-like nanoparticle layers on PDMS. (a) After AP-PECVD treatment. (b) After Parylene-C layer deposition on PDMS. (c) After the removal process of Parylene-C from PDMS using adhesive tape. Scale bars = 5 μm. (The wrinkles of the Parylene-C layer in (b) and (c) were not the original morphology of the sample; this was generated during SEM measurement.)

Table 1. Relative Chemical Composition Ratio of C, O, Si, and Cl in Each Sample Surface As Determined by XPS Analysis during the Removal Process of Parylene-C from PDMS

location[a]	description	relative chemical composition ratio (at %)			
		C	O	Si	Cl
@1	pristine PDMS	44.9	27.2	27.9	0.0
@2	AP-PECVD	27.8	42.9	29.3	0.0
@3	Parylene-C CVD	86.6	0.9	0.0	12.5
@4	RIE etching	31.2	38.8	30.0	0.0
@5	peeled-off tape from AP-PECVD-treated PDMS	76.4	9.8	4.5	9.3
@6	peeled-off PDMS (open area)	43.9	28.0	28.1	0.0
@7	peeled-off PDMS (closed area)	42.9	28.6	28.5	0.0
@8	Parylene-C CVD	85.8	2.7	1.0	10.5
@9	peeled-off PDMS	77.0	8.5	8.7	5.8
@10	peeled-off tape from glass	84.9	3.1	0.0	12.0

[a]The location of each surface is designated in Figure S3a, Supporting Information.

and the ratio of Cl, which originated from Parylene-C, changed from 12.5% to 0% after the removal process of the Parylene-C using adhesive tape. However, the chemical composition ratio of PDMS without AP-PECVD was markedly different from that of pristine PDMS, and the ratio of Cl remained after the removal process of the Parylene-C layer using adhesive tape. Thus, it could be inferred that the Parylene-C layer could be completely peeled away from the PDMS substrate by means of AP-PECVD of TEOS-O_2.

In Table 1, the chemical composition ratio of open areas (@6) and closed areas (@7) in PDMS from which Parylene-C had been peeled off after AP-PECVD was similar to that of pristine PDMS (@1), although there had been changes in the chemical composition ratio of the PDMS surface (@2) mediated by addition of SiOx-like nanoparticle layers via AP-PECVD prior to Parylene-C deposition. Removal of SiOx-like nanoparticle layers from the open area was achieved by BOE etchant. However, SiOx-like nanoparticle layers could not be removed from the closed area, given that it was covered by the Parylene-C layer, which resists chemical reaction with acids, alkalis, and solvents. To ascertain the location of the SiOx-like nanoparticle layers in the closed area, we compared the chemical composition ratio of the surface of adhesive tape (@5) peeled from Parylene-C-deposited PDMS that had undergone AP-PECVD with that of the surface of the adhesive tape (@10) peeled from a Parylene-C-deposited glass slide (considering the smooth peeling-off of the Parylene-C layer from a glass slide). The chemical composition ratio of the adhesive tape peeled from a Parylene-C-deposited glass slide (@10) was very similar to that of Parylene-C-deposited PDMS that had undergone AP-PECVD (@3) and that without AP-PECVD (@8); the chemical composition ratio of these surfaces were very similar given that their surfaces were fully covered with Parylene-C. However, there was a distinct difference between the chemical composition ratio of the adhesive tape peeled from Parylene-C-deposited PDMS with AP-PECVD (@5) and that peeled from Parylene-C-deposited glass (@10). Considering the presence of Cl, which originated from Parylene-C only, it appears that the Parylene-C layer was detached simultaneously by adhesive tape. However, the relative ratio of Si and O in adhesive tape containing the detached Parylene-C layer from PDMS that had

between PDMS and the Parylene-C layer containing SiOx-like nanoparticle layers, given that the latter prevented penetration of the Parylene-C into PDMS. We believe that the penetration of Parylene-C was prevented by a SiOx-like nanoparticle layer that blocks the nanopores on PDMS. We expect that a similar strategy to prevent the penetration of Parylene-C into nanopores of PDMS surface might be helpful to ensure reliable, complete removal of Parylene-C from PDMS.

3.4. Change in Relative Chemical Composition Ratio on the PDMS Surface. The detailed trends observed in changes of the relative chemical composition ratio on PDMS surfaces during the removal process of Parylene-C were investigated. Table 1 shows the variation in the relative chemical composition ratio in each step as determined by XPS analysis. Figure S3a, Supporting Information, describes each location of the PDMS sample surface as measured by XPS, and Figure S3b, Supporting Information, shows a graphical comparison of the relative chemical composition ratio. After the removal process of Parylene-C, the chemical composition ratios of open and closed areas on PDMS that had undergone AP-PECVD were markedly similar to those of pristine PDMS,

undergone AP-PECVD (@5) was higher than that in another adhesive tape containing separated Parylene-C layer from glass (@10), whereas the relative ratio of C and Cl was lower. On the basis of this difference in chemical composition ratio of two detached Parylene-C layers in adhesive tapes, we deduced that SiOx-like nanoparticle layers were detached from the PDMS surface along with Parylene-C during the removal process using adhesive tape, assuming a conformal coating given the gaseous nature of the deposition process of Parylene-C.

4. CONCLUSIONS

We have developed a patterning method on flexible PDMS substrates by mechanical removal of an on-chip Parylene-C microstencil using adhesive tape. Surface modification by AP-PECVD of TEOS-O$_2$ to deposit SiOx-like nanoparticle layers was essential to allow residue-free removal of the Parylene-C layer from PDMS, and the complete removal of Parylene-C using AP-PECVD was demonstrated by various surface characterization analysis. Utilizing the surface modification and photolithography, an on-chip parylene microstencil was realized for simple-to-use patterning of proteins and cells on PDMS. This approach demonstrated a capacity for high resolution and throughput with superior user-friendliness. Thus, this patterning method on flexible PDMS could be used in various applications such as micrototal analysis systems (μTAS) and tissue engineering.

■ ASSOCIATED CONTENT

Ⓢ Supporting Information

Quantitative analysis on the uniformity of patterning result; measured thickness of deposited layer on PDMS with variation in the number of AP-PECVD treatments; relative chemical composition ratios as determined by XPS analysis during the fabrication process of an on-chip Parylene-C microstencil and removal process of Parylene-C microstencil from PDMS. This information is available free of charge via the Internet at http://pubs.acs.org.

■ AUTHOR INFORMATION

Corresponding Author
*Address: #624, Dasan Bldg., 123 Cheomdan-gwagiro Buk-gu, Gwangju, 500-712, Republic of Korea. Phone: +82-62-715-2407. Fax: +82-62-715-2384. E-mail: syang@gist.ac.kr.

Author Contributions

The manuscript was written through contributions of all authors. All authors have approved the final version of the manuscript.

Notes

The authors declare no competing financial interest.

■ ACKNOWLEDGMENTS

■ ABBREVIATIONS

AP-PECVD = atmospheric pressure-plasma-enhanced chemical vapor deposition
ATR = attenuated total reflectance
CV = coefficient of variation
ECM = extracellular matrix
FBS = fetal bovine serum
FITC = fluorescein isothiocyanate
FTIR = fourier transform infrared spectroscopy
PDMS = polydimethylsiloxane
PLL = poly-L-lysine
PLL-FITC = FITC-labeled poly-L-lysine
RIE = reactive ion etching
SA-FITC = FITC-labeled streptavidin
sccm = standard cubic centimeter per minute
slm = standard liter per minute
TEOS = tetraethyl orthosilicate
UV−vis = ultraviolet−visible spectrophotometry
XPS = X-ray photoelectron spectroscopy

■ REFERENCES

(1) Gervais, L.; de Rooij, N.; Delamarche, E. *Adv. Mater.* **2011**, *23*, H151−H176.
(2) Kovarik, M. L.; Gach, P. C.; Ornoff, D. M.; Wang, Y. L.; Balowski, J.; Farrag, L.; Allbritton, N. L. *Anal. Chem.* **2012**, *84*, 516−540.
(3) Mu, X.; Zheng, W.; Sun, J.; Zhang, W.; Jiang, X. *Small* **2012**, *9*−21.
(4) Barbulovic-Nad, I.; Lucente, M.; Sun, Y.; Zhang, M.; Wheeler, A. R.; Bussmann, M. *Crit. Rev. Biotechnol.* **2006**, *26*, 237−259.
(5) Falconnet, D.; Csucs, G.; Grandin, H. M.; Textor, M. *Biomaterials* **2006**, *27*, 3044−3063.
(6) Velve-Casquillas, G.; Le Berre, M.; Piel, M.; Tran, P. T. *Nano Today* **2010**, *5*, 28−47.
(7) Chang, T. Y.; Yadav, V. G.; De Leo, S.; Mohedas, A.; Rajalingam, B.; Chen, C. L.; Selvarasah, S.; Dokmeci, M. R.; Khademhosseini, A. *Langmuir* **2007**, *23*, 11718−11725.
(8) Lee, J. N.; Park, C.; Whitesides, G. M. *Anal. Chem.* **2003**, *75*, 6544−6554.
(9) Lei, Y. H.; Liu, Y. P.; Wang, W.; Wu, W. G.; Li, Z. H. *Lab Chip* **2011**, *11*, 1385−1388.
(10) Renault, J. P.; Bernard, A.; Juncker, D.; Michel, B.; Bosshard, H. R.; Delamarche, E. *Angew. Chem.* **2002**, *114*, 2426−2429.
(11) Chiu, D. T.; Jeon, N. L.; Huang, S.; Kane, R. S.; Wargo, C. J.; Choi, I. S.; Ingber, D. E.; Whitesides, G. M. *Proc. Natl. Acad. Sci. U. S. A.* **2000**, *97*, 2408−2413.
(12) Delamarche, E.; Bernard, A.; Schmid, H.; Michel, B.; Biebuyck, H. *Science* **1997**, *276*, 779−781.
(13) Atsuta, K.; Noji, H.; Takeuchi, S. *Lab Chip* **2004**, *4*, 333−336.
(14) Jinno, S.; Moeller, H. C.; Chen, C. L.; Rajalingam, B.; Chung, B. G.; Dokmeci, M. R.; Khademhosseini, A. *J. Biomed. Mater. Res., Part A* **2008**, *86A*, 278−288.
(15) Wright, D.; Rajalingam, B.; Selvarasah, S.; Dokmeci, M. R.; Khademhosseini, A. *Lab Chip* **2007**, *7*, 1272−1279.
(16) Wright, D.; Rajalingam, B.; Karp, J. M.; Selvarasah, S.; Ling, Y.; Yeh, J.; Langer, R.; Dokmeci, M. R.; Khademhosseini, A. *J. Biomed. Mater. Res., Part A* **2008**, *85A*, 530−538.
(17) Selvarasah, S.; Chao, S. H.; Chen, C. L.; Sridhar, S.; Busnaina, A.; Khademhosseini, A.; Dokmeci, M. R. *Sens. Actuators, A* **2008**, *145*−*46*, 306−315.
(18) Huang, M.; Galarreta, B. C.; Artar, A.; Adato, R.; Aksu, S.; Altug, H. *Nano Lett.* **2012**, *12*, 4817−4822.
(19) Pataky, K.; Cordey, M.; Brugger, J.; Lutolf, M. *Eur. Cells Mater.* **2007**, *14*, 109.
(20) Vazquez-Mena, O.; Sannomiya, T.; Tosun, M.; Villanueva, L. G.; Savu, V.; Voros, J.; Brugger, J. *ACS Nano* **2012**, *6*, 5474−5481.
(21) Paik, I.; Scurr, D. J.; Morris, B.; Hall, G.; Denning, C.; Alexander, M. R.; Shakesheff, K. M.; Dixon, J. E. *Biotechnol. Bioeng.* **2012**, *109*, 2630−2641.
(22) Qin, D.; Xia, Y.; Whitesides, G. M. *Nat. Protoc.* **2010**, *5*, 491−502.
(23) Tan, C. P.; Ri Seo, B.; Brooks, D. J.; Chandler, E. M.; Craighead, H. G.; Fischbach, C. *Integr. Biol.* **2009**, *1*, 587−594.

(24) Tan, C. P.; Cipriany, B. R.; Lin, D. M.; Craighead, H. G. *Nano Lett.* **2010**, *10*, 719−725.

(25) Chen, H. Y.; Elkasabi, Y.; Lahann, J. *J. Am. Chem. Soc.* **2006**, *128*, 374−380.

(26) Flueckiger, J.; Bazargan, V.; Stoeber, B.; Cheung, K. C. *Sens. Actuators, B* **2011**, *160*, 864−874.

(27) Sasaki, H.; Onoe, H.; Osaki, T.; Kawano, R.; Takeuchi, S. *Sens. Actuators, B* **2010**, *150*, 478−482.

(28) Lee, D.; Yang, S. *Sens. Actuators, B* **2012**, *162*, 425−434.

(29) Rogers, J. A.; Someya, T.; Huang, Y. G. *Science* **2010**, *327*, 1603−1607.

(30) Moraes, C.; Sun, Y.; Simmons, C. A. *Integr. Biol.* **2011**, *3*, 959−971.

(31) Ekblad, T.; Liedberg, B. *Curr. Opin. Colloid Interface Sci.* **2010**, *15*, 499−509.

(32) Bayiati, P.; Malainou, A.; Matrozos, E.; Tserepi, A.; Petrou, P. S.; Kakabakos, S. E.; Gogolides, E. *Biosens. Bioelectron.* **2009**, *24*, 2979−2984.

(33) Moran-Mirabal, J. M.; Tan, C. P.; Orth, R. N.; Williams, E. O.; Craighead, H. G.; Lin, D. M. *Anal. Chem.* **2006**, *79*, 1109−1114.

(34) Petrou, P. S.; Chatzichristidi, M.; Douvas, A. M.; Argitis, P.; Misiakos, K.; Kakabakos, S. E. *Biosens. Bioelectron.* **2007**, *22*, 1994−2002.

(35) Hwang, H.; Kang, G.; Yeon, J. H.; Nam, Y.; Park, J. K. *Lab Chip* **2009**, *9*, 167−170.

(36) Park, J. Y.; Takayama, S.; Lee, S.-H. *Integr. Biol.* **2010**, *2*, 229−240.

(37) El-Ali, J.; Sorger, P. K.; Jensen, K. F. *Nature* **2006**, *442*, 403−411.

(38) Simmons, C. S.; Petzold, B. C.; Pruitt, B. L. *Lab Chip* **2012**, *12*, 3235−3248.

(39) Kilian, K. A.; Bugarija, B.; Lahn, B. T.; Mrksich, M. *Proc. Natl. Acad. Sci. U. S. A.* **2010**, *107*, 4872−4877.

(40) McBeath, R.; Pirone, D. M.; Nelson, C. M.; Bhadriraju, K.; Chen, C. S. *Dev. Cell* **2004**, *6*, 483−495.

(41) Huh, D.; Fujioka, H.; Tung, Y. C.; Futai, N.; Paine, R.; Grotberg, J. B.; Takayama, S. *Proc. Natl. Acad. Sci. U. S. A.* **2007**, *104*, 18886−18891.

(42) Alf, M. E.; Asatekin, A.; Barr, M. C.; Baxamusa, S. H.; Chelawat, H.; Ozaydin-Ince, G.; Petruczok, C. D.; Sreenivasan, R.; Tenhaeff, W. E.; Trujillo, N. J.; Vaddiraju, S.; Xu, J. J.; Gleason, K. K. *Adv. Mater.* **2010**, *22*, 1993−2027.